Design and Development of a 26-Pole and 24-Slot Bearingless Motor

Franz Zürcher[1], Thomas Nussbaumer[2], Wolfgang Gruber[3], and Johann W. Kolar[1]

Power Electronic Systems Laboratory, ETH Zurich,Zurich, Switzerland
Levitronix GmbH, Zurich, Switzerland
ACCM GmbH (Johannes Kepler Universität Linz), Zurich, Austria

Several processes in chemical, pharmaceutical, biotechnology and semiconductor industry require contactless levitation and rotation through a hermetically closed process chamber. A highly interesting topology for these applications is the "bearingless slice motor" concept, where already some research has been done in the past. This paper presents the design, optimization and development of a 26-pole and 24-slot bearingless motor, which promises high acceleration and bearing performance and an ultra-compact setup. A prototype with a large rotor diameter and a large air-gap has been built to verify the simulation results by experiments.

***Index Terms*—AC motor drives, bearingless slice motors, magnetic levitation, permanent magnet motors, synchronous machines.**

I. Introduction

NOWADAYS, several processes in the chemical, pharmaceutical and semiconductor industry are demanding for ultra-clean environments [1]. In these applications, bearingless motors offer a good possibility to guarantee a high cleanness, since no particles are produced by wear of friction and no lubricants are needed. By contactless levitation and rotation through an enclosure the process can be hermetically encapsulated from the drive and bearing electronics. Even though these motors are characterized by higher costs due to complicated assembly and control they are frequently employed in the aforementioned areas due to their superior performance. Several different setups for bearingless motors have been presented so far, such as bearingless induction machines [2], consequent-pole-type bearingless motors [3], switched reluctance bearingless motors [4], bearingless brushless DC motors [5] and bearingless slice motors with homopolar bearings [6].

Advanced concepts with high pole numbers have been proposed, which achieve superior performance results, such as a 8-pole 12-slot bearingless motor in [7], a 16-pole slotless self-bearing motor in [8] or a multi-consequent-pole bearingless motor in [9]. This paper presents the design and development of a new bearingless motor with 26 rotor poles and 24 slots, which is highly interesting for a large rotor diameter and large air gap. The proposed concept guarantees a very high level of compactness and superior suspension and torque performance, which is achieved by the specific fractional slot/pole ratio along with an appropriate winding scheme.

As known from literature, a fractional ratio x_q of the number of stator-teeth q (which is equal to the number of stator slots) and the number of poles $2p$ [10] can be used to reduce the cogging torque of synchronous machines practically without limiting the drive torque [11]–[13]. However, these asymmetric winding configurations often produce undesirable radial forces [14] in conventional machines, which result in stresses on the mechanical bearings. The proposed bearingless motor concept takes advantage of this fractional ratio to intentionally control the suspension forces in addition to the motor torque in a decoupled manner. If appropriate winding configurations for the drive and bearing units are chosen, a highly compact setup with excellent performance can be achieved with this concept. This bearingless motor concept can be used to actively control three degrees of freedom of a rotor: the deflections along the two radial axes of the rotor x and y and the rotation angle α. By using an auxiliary passive bearing (cf. slice motor concept [6]) or by combining two of these stator elements and an additional thrust-bearing (cf. bearingless canned motor [15] and [16]) the remaining three degrees of freedom, namely the tilting angles φ_x and φ_y and the deflection along the axial direction z, can be stabilized.

II. Principles of the Bearingless Motor Concept

The proposed bearingless motor consists of a stator, which holds the bearing and drive windings as well as the position and angular sensors, and a rotor with $2p$ permanent magnets. Three degrees of freedom are controlled actively, namely the radial displacement Δx and Δy by the bearing windings and the rotational angle α by the drive windings. The remaining three degrees of freedom, the tilting angles φ_x and φ_y and the axial deflection Δz, are stabilized passively by reluctance forces of the bearingless slice motor, as proposed in [6]. This allows a very compact setup, as no additional thrust bearing is needed and the maximal height of the bearingless motor is therefore given by the stator height h. Although the bearing and drive units can be integrated on the same stator, the drive torque T_D and the bearing forces F_x and F_y can be controlled in a decoupled manner, as will be shown.

The key parameters of the setup are the number of stator teeth/slots q, the number of rotor poles $2p$ and the fractional ratio x_q of these two parameters, respectively

$$x_q = \frac{q}{p} \tag{1}$$

as well as the number of drive and bearing phases m_{drv} and m_{bng}, respectively. Each of the q stator teeth carries either a drive winding or a bearing winding, whereby only concentrated windings in an alternating drive/bearing sequence are considered in this paper. With this, the winding configurations for both drive and bearing windings can be chosen in dependence on parameters q, p, m_{drv} and m_{bng}.

Manuscript received March 06, 2009; revised April 23, 2009. Current version published September 18, 2009. Corresponding author: F. Zürcher (e-mail: zurcher@ieee.org).

Color versions of one or more of the figures in this paper are available online at http://ieeexplore.ieee.org.

Digital Object Identifier 10.1109/TMAG.2009.2024216

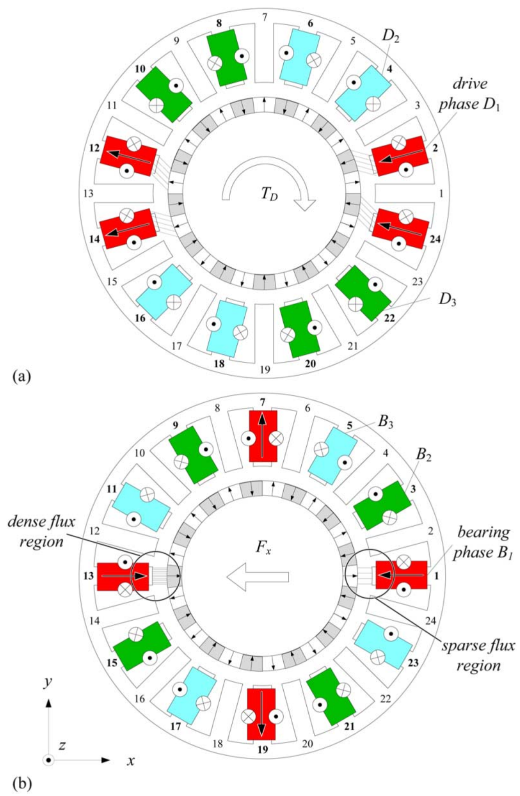

Fig. 1. Motor (a) and bearing (b) winding concept of the bearingless slice motor with q = 24 slots and p = 13 pole-pairs.

A. Permanent Magnet Synchronous Drive

As known from literature the unwanted cogging torque can be reduced by choosing a fractional ratio x_q of the number of stator teeth/slots and the number of rotor pole-pairs [11], [12]. If an appropriate drive winding scheme is chosen, a resulting drive torque T_D can be achieved by applying a current with a 90 degree phase shift with respect to the permanent magnet flux in the corresponding drive phase, as known from state-of-the-art field orientated control for permanent magnet synchronous machines. This is shown exemplarily in Fig. 1(a). The parasitic radial forces generated by the drive currents can never produce a resulting displacement force, as the parasitic radial forces generated by the two opposite stator teeth cancel each other, if the rotor with the permanent magnets and the stator with the windings are designed perfectly symmetrical, as depicted in Fig. 1(a). The resulting drive torque T_D can be calculated by the simplified equation

$$T_D = \frac{m_{\mathrm{drv}}}{2} \cdot k_T \cdot N_{\mathrm{drv}} \cdot \hat{I}_{\mathrm{drv}} \qquad (2)$$

where k_T is the torque-current-factor, N_{drv} the number of drive windings per phase, $\hat{I}_{\mathrm{drv}}$ the peak current of the m_{drv} drive phases.

B. Active Radial Magnetic Bearing

For an appropriate combination of q and p, the rotor permanent magnets are perfectly aligned to the stator teeth front faces. The suspension forces F_x and F_y can be generated by an appropriate winding scheme (being different from the drive winding scheme), where the opposite stator teeth carry reverse windings. Therefore, the radial forces generated by the currents of one of the m_{bng} bearing phases do not cancel each other but summarize, because they point into the same direction, as depicted in Fig. 1(b). On the other hand, the bearing windings can never produce a resulting torque for any angular rotor position. For the symmetrical case, the levitation force component F_x in radial x-direction can be calculated by

$$F_x(\delta) = \frac{m_{\mathrm{bng}}}{2} \cdot k_F \cdot N_{\mathrm{bng}} \cdot \hat{I}_{\mathrm{bng}} \cdot \cos(\delta) \qquad (3)$$

where k_F is the force-current-factor, N_{bng} the number of drive windings per phase, $\hat{I}_{\mathrm{bng}}$ the peak value of the ac currents $i_{\mathrm{bng}}(\alpha)$ in each of the m_{bng} bearing phases with a phase shift of 360 deg/m_{bng} and δ the angle of the desired force with respect to the x-axis. The force component F_y in y-direction can be calculated analogously. Since the phase currents depend on the angular rotor position α, this angle has to be measured precisely to control the direction of the resulting bearing force. Experiments have shown, that for stable operation the measured angular position must not differ more than ±20 electrical degrees.

The radial displacement force F_r caused by the negative radial stiffness k_r according to

$$F_r = \Delta r \cdot k_r \qquad (4)$$

has to be counteracted actively by appropriate bearing forces F_x and F_y. The following equation has to be fulfilled in order to guarantee a stable operation of the active magnetic bearing in radial direction within the maximal allowed radial deflection $\Delta r_{\max}$

$$k_F > \frac{k_r \cdot \Delta r_{\max}}{N_{\mathrm{bng}} \cdot I_{\mathrm{bng}}}. \qquad (5)$$

For a stable passive bearing in z-direction, also the following equation has to be fulfilled:

$$k_z > \frac{m \cdot g}{\Delta z} \qquad (6)$$

where m is the rotor weight and Δz the maximal allowed axial deflection of the rotor. A similar condition must be fulfilled for the passive tilting forces with the tilting stiffness k_φ and the maximal allowed tilting angle $\Delta\varphi$.

III. Specific System Parameters and Winding Concept

The key parameters of the system discussed in this paper have been chosen as following: the number of stator teeth $q = 24$, the number of rotor permanent magnets $2p = 26$, the number of bearing and drive phases $m_{\mathrm{bng}} = 3$ and $m_{\mathrm{drv}} = 3$. Different concepts have been analyzed, but the above mentioned topology has emerged as the most promising one in sake of drive and bearing performance and control effort for the intended maximal rotational speed of $n_{r,\max} = 1500$ r/min and the target outer diameter of the system $d_{\mathrm{stator}} = 500$ mm, and a mechanical air-gap of $\delta = 7$ mm.

Fig. 1(a) shows the drive winding concept for the chosen parameters q, p and m_{drv}. The flux is equally attenuated or amplified in the two opposite air-gaps, therefore no radial force is resulting, for any currents in the drive phases D_1, D_2 and D_3. This reduces the controlling effort, as no parasitic radial forces, which could influence the bearing have to be considered in the

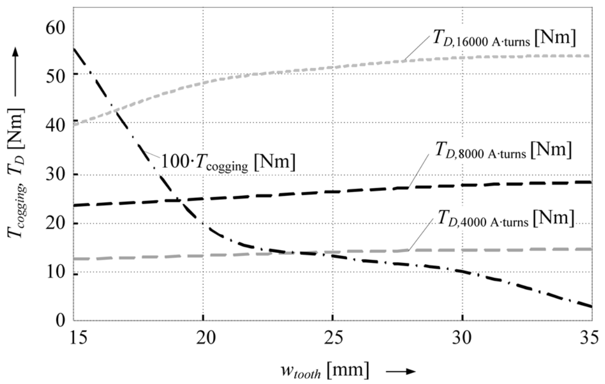

Fig. 2. Influence of the stator tooth width w_{tooth} on the cogging torque T_{cogging} and the drive torque T_D for different ampere-turns.

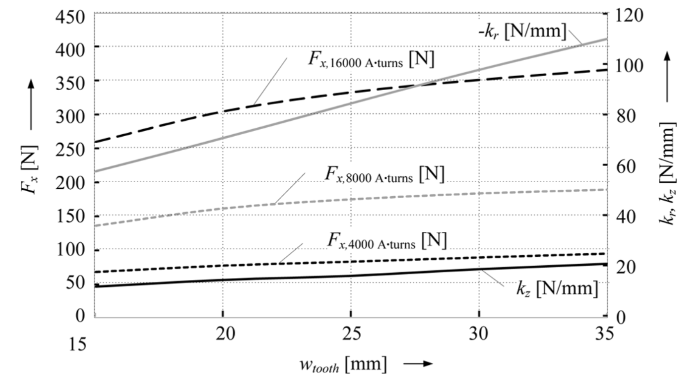

Fig. 3. Influence of the stator tooth width w_{tooth} on the radial and axial stiffness k_r and k_z, and the suspension force F_x for different ampere turns.

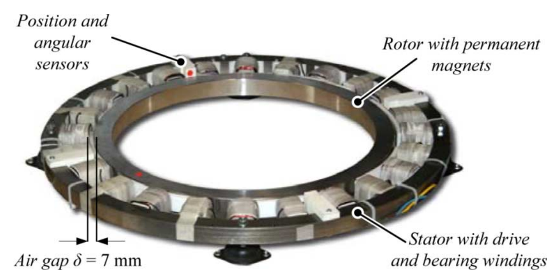

Fig. 4. Photo of the experimental prototype.

drive controlling scheme. Thus the control of the drive system is a state-of-the-art field-oriented control of the permanent magnet synchronous machine.

Fig. 1(b) shows how a radial suspension force F_x can be generated by applying a current in the bearing windings for the specific system with q, p and m_{bng}. For the depicted exemplary situation with the angular rotor position α and a bearing current I_{bng} applied to phase B_1 (wound around the stator teeth 1, 7, 13 and 19), a radial force F_x in negative x-direction is resulting. The magnetic flux generated by the current in the phase B_1 in the right sided stator tooth 1 weakens the permanent magnet flux in the air-gap, while in front on the opposite tooth 13 the flux generated by the current in phase B_1 accumulates to the permanent magnet flux. Therefore, a region of dense air-gap flux is generated on the left side while a sparse flux region is generated in the air-gap on the right side, thus a radial force is resulting towards the left side. With this, a suspension force in any desired direction can be achieved for every possible angular rotor position by air-gap-flux oriented control of the three bearing phase currents B_1, B_2, and B_3. An appropriate control scheme is given in [17].

IV. Parameter Optimization

After choosing a system topology with the key parameters q, p, m_{bng} and m_{drv} the remaining design parameters have to be defined, namely the radial magnet length l_{magnet}, the stator and rotor height h and the stator tooth-width w_{tooth}. These design parameters can be found by optimization through simulation tools. The goal of the optimization here is to find a parameter set with optimal acceleration and bearing performance, which means maximizing the drive torque T_D and the bearing forces F_x and F_y as well as the axial stiffness k_z and the tilting stiffness k_φ, while the radial stiffness k_r should be minimized.

3D-FEM simulations for all these design parameters have been undertaken to find an optimal design. Fig. 2 shows exemplarily the influence of the stator tooth width w_{tooth} on the performance parameters drive torque T_D and cogging torque T_{cogging}. Simulations with w_{tooth} varying from 15 mm to 35 mm have been undertaken for different ampere-turns, whereby the number of drive windings N_{drv} per phase has been optimized to minimize the acceleration time $t_{\mathrm{acc},0-1500}$ in each case (since sufficient stator space is available, the current densities of the windings in the stator slots are not the limiting parameter). It can be seen that the drive torque T_D is increasing with increasing tooth width, while the unwanted cogging torque T_{cogging} is decreased. For tooth widths above 25 mm the drive torque can no longer be increased significantly. Similar simulations for the bearing performance have been made for the same values of w_{tooth}. In Fig. 3 it can be seen that by increasing w_{tooth}, both the negative radial and positive axial stiffness are increased. The increased radial stiffness has to be counteracted by higher levitation forces, which are also increasing with w_{tooth} for a specific number of ampere-turns. Apparently, k_r has a stronger rise than the levitation force F_x. From this point of view, a smaller value of w_{tooth} seems to be preferable for the bearing stability, which is contradictory to the w_{tooth} for optimal drive performance. As a compromise, for the prototype the stator tooth width has been chosen as $w_{\mathrm{tooth}} = 20$ mm, as this promises a high torque as well as a high axial stiffness and a reasonable low radial stiffness.

Similar simulations have been made to find optimal values of the stator height h_{stator} and the radial magnet length l_{magnet}. The chosen values are given in Table I.

V. Experimental Performance of the Prototype

A laboratory prototype with the optimized design parameters has been built, which is depicted in Fig. 4, where also the most important parts are labeled. Also the most important achieved performance results are given at the end of Table I, and compared to the simulated values.

For a maximal drive current $I_{\mathrm{drv,max,RMS}} = 10$ A, acceleration from 0 r/min to 1500 r/min lasts 1510 ms, which is in very good accordance to the analytically calculated value (1495 ms) based on simulation results of the drive torque. Fig. 5 shows the drive and bearing currents I_{drv} and I_{bng} of one phase and the radial deflection Δr during acceleration and deceleration. The

TABLE I
PROPERTIES AND PARAMETERS OF THE LABORATORY PROTOTYPE

parameter	symbol	value[1]	value[2]	unit
Number of stator teeth / slots	q	24		
Number of drive teeth	q_{drv}	12		
Number of bearing teeth	q_{bng}	12		
Number of rotor poles	$2p$	26		
Number of bearing phases	m_{bng}	3		
Number drive phases	m_{drv}	3		
Number of drive windings	N_{drv}	200		turns/phase
Number of bearing windings	N_{bng}	400		turns/phase
Maximum rotational speed	$n_{r,max}$	1500		r/min
Stator tooth width	w_{tooth}	20		mm
Permanent magnet length	l_{magnet}	20		mm
Stator iron height	h_{stator}	20		mm
Stator outer diameter	d_{stator}	500		mm
Rotor weight	m_{rotor}	4.2		kg
Mechanical air-gap	δ	7		mm
Axial stiffness	k_z	20.1		N/mm
Tilting stiffness	k_φ	4.7		Nm/deg
Radial stiffness	k_r	70.0	75.9	N/mm
Force-current factor	k_F	18.5	25.8	mN/(A·turns)
Torque-current factor	k_T	3.1		mNm/(A·turns)
Acceleration time	$t_{acc,0\text{-}1500}$	1495	1510	ms
Rated torque	T_D	13.1		Nm
Rated drive current	$I_{D,\mathrm{rms}}$	10		A
Maximum power	P_{max}	1.6		kW
Maximum bearing force	F_{max}	155		N
Ang. pos. sensor accuracy	$\Delta\,\alpha$	±3.5		electrical deg

value[1] gained from 3D-FEM simulations and value[2] gained from experimental results of the laboratory prototype

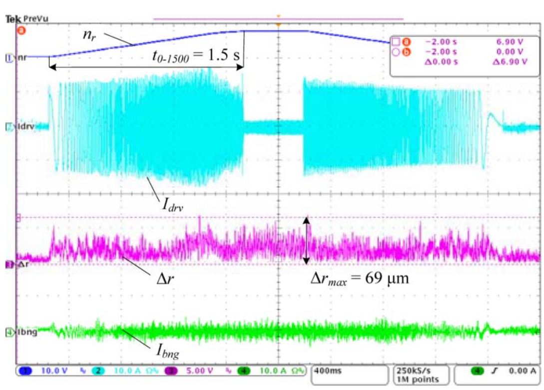

Fig. 5. Acceleration and bearing performance of the prototype from 0 r/min to 1500 r/min. (scales: CH1: n_r, 2000 r/min/div, CH2: I_{drv}, 10 A/div, CH3: Δr, 50 μm/div, CH4: I_{bng}, 10 A/div.).

maximal radial deflection of 69 μm during acceleration is acceptable for the intended applications in process industry and in standstill it is even smaller than 10 μm.

VI. Conclusion

This paper describes a new bearingless motor with 26 rotor poles and 24 stator slots, which is of high interest for several industry branches, where spin processes in a high-purity environment have to be performed. The proposed concept features high acceleration capability and an ultra-compact setup with low control effort. In this paper, the functionality of the magnetic bearing and the permanent magnet synchronous drive is explained and guidelines for the optimization of the design are presented. Finally, the theoretical considerations and simulation results have been verified by measurements of the achievable bearing and acceleration performance on a prototype.

References

[1] Y. Chisti and M. Moo-Young, "Clean-in-place systems for industrial bioreactors: Design, validation and operation," *J. Industr. Microbiol. Biotechnol.*, vol. 13, pp. 201–207, Jul. 1994.

[2] A. Chiba, D. Power, and M. Rahman, "Characteristics of a bearingless induction motor," *IEEE Trans. Magn.*, vol. 27, pt. 6, pp. 5199–5201, Nov. 1991.

[3] J. Amemiya, A. Chiba, D. Dorrell, and T. Fukao, "Basic characteristics of a consequent-pole-type bearingless motor," *IEEE Trans. Magn.*, vol. 41, no. 1, pp. 82–89, Jan. 2005.

[4] G. Yang, Z. Deng, X. Cao, and X. Wang, "Optimal winding arrangements of a bearingless switched reluctance motor," *IEEE Trans. Power Electron.*, vol. 23, no. 6, pp. 3056–3066, Nov. 2008.

[5] M. Ooshima, "Winding arrangement to increase suspension force in bearingless motors with brushless DC structure," in *Proc. IEEE IECON Conf.*, 2007, pp. 181–186.

[6] P. Karutz, T. Nussbaumer, W. Gruber, and J. W. Kolar, "Novel magnetically levitated two-level motor," *IEEE/ASME Trans. Mechatron.*, vol. 13, no. 6, pp. 658–668, Nov. 2008.

[7] M. Ooshima, "Analyses of rotational torque and suspension force in a permanent magnet synchronous bearingless motor with short-pitch winding," in *Proc. IEEE Power Eng. Society General Mtng*, 2007, pp. 1–7.

[8] L. S. Stephens and D. Kim, "Analysis and simulation of a Lorentz-type slotless, self-bearing motor," *Control Eng.Practice*, vol. 10, pp. 899–905, Aug. 2002.

[9] N. Watanabe, H. Sugimoto, A. Chiba, T. Fukao, and M. Takemoto, "Basic characteristic of the multi-consequent-pole bearingless motor," in *Proc. PCC*, Nagura, 2007, pp. 1565–1570, und.

[10] M. Ahmad, N. Manap, and D. Ishak, "Permanent magnet brushless machines with minimum difference in slot number and pole number," in *Proc. IEEE PECon*, 2008, pp. 1064–1069.

[11] C. Hwang, M. Wu, and S. Cheng, "Influence of pole and slot combinations on cogging torque in fractional slot PM motors," *J. Magn. Magn. Mater.*, vol. 304, pp. e430–e432, Sep. 2006.

[12] Y. Chen, Z. Zhu, and D. Howe, "Vibration of PM brushless machines having a fractional number of slots per pole," *IEEE Trans. Magn.*, vol. 42, no. 11, pp. 3395–3397, Nov 2006.

[13] T. Jahns and W. Soong, "Pulsating torque minimization techniques for permanent magnet AC motor drives-a review," *IEEE Trans. Ind. Electron.*, vol. 43, no. 1, pp. 321–330, Feb. 1996.

[14] F. Magnussen and H. Lendenmann, "Parasitic effects in PM machines with concentrated windings," *IEEE Trans. Ind. Appl.*, vol. 43, no. 10, pp. 1223–1232, Oct. 2007.

[15] C. Redemann, P. Meuter, A. Ramella, and T. Gempp, "Development and prototype of a 30 kW bearingless canned motor pump," in *Proc. IPEC*, Tokyo, Japan, 2000, pp. 377–382.

[16] Q. Hijikata, S. Kobayashi, M. Takemoto, Y. Tanaka, A. Chiba, and T. Fukao, "Basic characteristics of an active thrust magnetic bearing with a cylindrical rotor core," *IEEE Trans. Magn.*, vol. 44, no. 12, pp. 4167–4170, Dec. 2008.

[17] T. Suzuki, A. Chiba, M. A. Rahman, and T. Fukao, "An air-gap-flux-oriented vector controller for stable operation of bearingless induction motors," *IEEE Trans. Ind. Appl.*, vol. 36, no. 4, pp. 1069–1076, Apr. 2000.